SCIENTIFIC REPORTS

OPEN

Thermal electron-tunneling devices as coolers and amplifiers

Shanhe Su[1,2], Yanchao Zhang[1], Jincan Chen[1] & Tien-Mo Shih[1,3]

Received: 29 October 2015
Accepted: 25 January 2016
Published: 19 February 2016

Nanoscale thermal systems that are associated with a pair of electron reservoirs have been previously studied. In particular, devices that adjust electron tunnels relatively to reservoirs' chemical potentials enjoy the novelty and the potential. Since only two reservoirs and one tunnel exist, however, designers need external aids to complete a cycle, rendering their models non-spontaneous. Here we design thermal conversion devices that are operated among three electron reservoirs connected by energy-filtering tunnels and also referred to as thermal electron-tunneling devices. They are driven by one of electron reservoirs rather than the external power input, and are equivalent to those coupling systems consisting of forward and reverse Carnot cycles with energy selective electron functions. These previously-unreported electronic devices can be used as coolers and thermal amplifiers and may be called as thermal transistors. The electron and energy fluxes of devices are capable of being manipulated in the same or oppsite directions at our disposal. The proposed model can open a new field in the application of nano-devices.

Numerous nanoscale studies that are related to harnessing thermal energy focus on pioneering concepts, fundamental principles, and unexplored mechanisms. They are exemplified by photosynthesis[1,2], quantum heat engines[3,4], spin-Seebeck power devices[5], thermal rectifiers[6–8], and Brownian motors[9]. Here, we consider a practically-functional device that consists of three electron reservoirs maintained at temperatures, T_h, T_c, and T_m as well as at chemical potentials, μ_h, μ_c, and μ_m [Fig. 1(a)], where distributions of electrons filled within these reservoirs obey Fermi-Dirac (FD) statistics, $f(\varepsilon, \mu, T)$[10,11]. These three reservoirs, connected by energy filtering tunnels serving heating, pumping, and feedback functions, establish a continuous cycle [Fig. 1(b,c)]. Such a three-terminal device has functions similar to thermal transistors. The first model of the thermal transistor to control heat flow was proposed by Li *et al.* using Frenkel-Kontorova FK lattices[12,13]. Prior to the analysis, let us first define the energy level at the intersection of two given FD distributions as E^*, yielding E_{hc}^*, E_{mc}^*, and E_{mh}^*[14,15], which denote reversible electron-transport energy levels between each pair of reservoirs. By adjusting three energy levels E_{hc}, E_{mc}, and E_{mh} relatively to these three starred levels, we are able to determine the directions of electron fluxes and achieve multiple purposes, namely, cooling and thermal amplification.

Results

The thermal devices are designed to remove q_c from the cold reservoir such that the cold reservoir is maintained at the cold temperature, T_c, and deliver thermal energy, q_m, to the median reservoir. To achieve these purposes, we use q_h as the power source in substitution of the electrical power. Note that q_h and q_c are net positive quantities exiting hot and cold reservoirs, whereas q_m is a net positive quantity entering the median reservoir. The center circle in Fig. 1(a) represents the equivalent results of the thermal energy transportation. In Fig. 1(b), the electron flux, n_{ij}, traveling through the tunnel between two given reservoirs, can be computed by Landauer equation[16,17] as

$$n_{ij} = \frac{2e}{h}\int_{E_{ij}-\Delta E/2}^{E_{ij}+\Delta E/2}[f(\varepsilon, \mu_i, T_i) - f(\varepsilon, \mu_j, T_j)]\,d\varepsilon, \tag{1}$$

where $\{i, j\} = \{h, c\}$, $\{c, m\}$, or $\{m, h\}$. Alternatively, we can write $\{i, j\} = \{c, h\}$, $\{h, m\}$, and $\{m, c\}$[Fig. 1(c)]. The pre-factor 2 accounts for the degeneracy of electrons; e the elementary charge; and h the Planck constant. Because the continuity of the electron flux requires that $n_{ch} = n_{hm} = n_{mc}$, three electron fluxes and thermal energy depend on each other. For example, the change of μ_h and T_h of the hot reservoir will affect the electron flux

[1]Department of Physics, Xiamen University, Xiamen 361005, People's Republic of China. [2]Beijing Computational Science Research Center, Beijing 100084, People's Republic of China. [3]Institute for Complex Adaptive Matter, University of California, Davis, CA 95616, USA. Correspondence and requests for materials should be addressed to J.C. (email: jcchen@xmu.edu.cn) or T.-M.S. (email: tshih111@gmail.com)

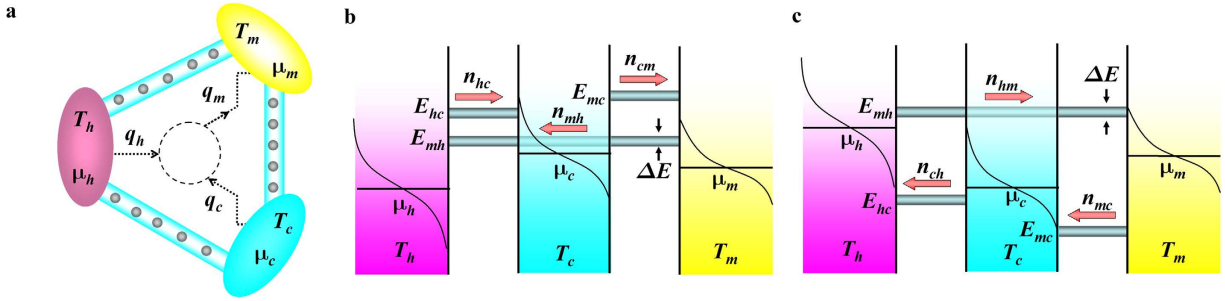

Figure 1. System schematics. (**a**) Thermal electron-tunneling devices that can serve dual purposes of cooling and amplification spontaneously with $T_h > T_m > T_c$; The thermal energy, q_h, exits from the hot reservoir, and is used as a power source, which allows the thermal energy, q_c, to be released from the cold reservoir, and lets the thermal energy, q_m, be pumped to the median reservoir. (**b**) For $\mu_c > \mu_h$, electron and thermal fluxes flow in the same direction with E_{mh} being the lowest tunnel energy level. (**c**) For $\mu_c < \mu_h$, electron and thermal fluxes flow in the opposite direction with E_{mh} being the highest tunnel energy. Red arrows in (**b**,**c**) indicate directions of electron fluxes.

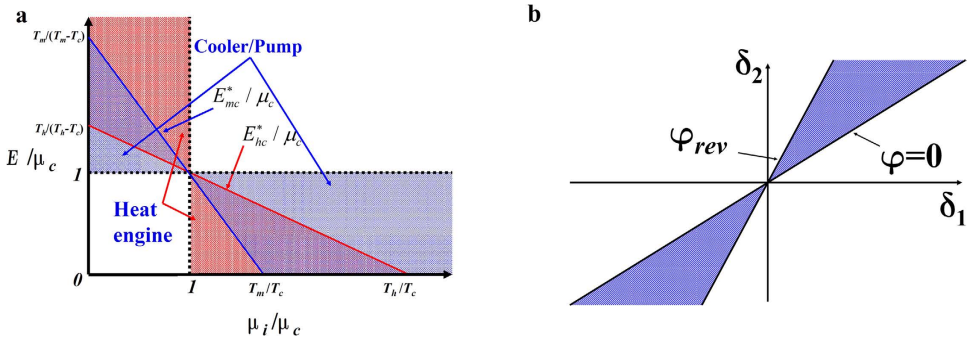

Figure 2. Regime diagrams. (**a**) The operable regime defined by the abscissa μ_i/μ_c ($i = h$ or m) and the ordinate E/μ_c. (**b**) Topography of the operable regime for the proposed device.

and thermal energy between the cold and median reservoir. Each electron leaving or entering a reservoir will carry away or inject the thermal energy equaling the difference between its kinetic energy and chemical potential[18–20]. The electron tunneling can now be realized in a semiconductor nanowire with double-barrier resonant-tunneling structure[19]. The energy levels of the all tunnels can be tuned by adjusting the barrier and well widths of the nanowire heterostructure. The thermal flux, q_h, associated with electron fluxes n_{hc} and n_{mh} can be obtained from Eq. (1) by inserting $\varepsilon - \mu_h$ in the integrand[21–23] and deleting e as

$$q_h = \frac{2}{h}\int_{E_{hc}-\Delta E/2}^{E_{hc}+\Delta E/2}(\varepsilon-\mu_h)[f_h(\varepsilon)-f_c(\varepsilon)]d\varepsilon - \int_{E_{mh}-\Delta E/2}^{E_{mh}+\Delta E/2}(\varepsilon-\mu_h)[f_m(\varepsilon)-f_h(\varepsilon)]d\varepsilon. \quad (2)$$

Likewise, we can calculate q_c and q_m using equations similar to Eq. (2). Temperatures considered here lie in the cryogenic range, so that we can neglect the lattice-related thermal conduction[24–26] and focus on electron kinetic energies[27,28].

Figure 2(a) represents a regime diagram defined by the abscissa μ_i/μ_c ($i = h$ or m) and the ordinate E/μ_c, which can be used to outline the principle of controlling electron-flux directions. Worth noting are four lines, namely, vertical dotted, horizontal dotted, red, and blue lines that represent, respectively, $\mu_i/\mu_c = 1$, $E/\mu_c = 1$, $E^*_{hc}/\mu_c = (T_h - T_c\mu_h/\mu_c)/(T_h - T_c)$, and $E^*_{mc}/\mu_c = (T_m - T_c\mu_m/\mu_c)/(T_m - T_c)$. Between hot and cold reservoirs, above the red line and left to the vertical dotted line lies the regime suitable for electron and thermal fluxes moving in the same direction from hot to cold reservoirs; below the red line and right to the vertical dotted line lies the regime suitable for counter flows (hot → cold for energy fluxes and cold → hot for electron fluxes). Between the cold reservoir and the median reservoir, below the blue line and above the horizontal dotted line lies the regime suitable for electron and thermal fluxes traveling from cold to median reservoirs; below the horizontal dotted line and above the blue line lies the regime suitable for counter flows (cold → median for energy fluxes and median → cold for electron fluxes). The vertical dotted line divides the diagram into two regimes: same-direction flows to the left, and counter flows to the right. According to Fig. 2 and analyses above, the systems shown in Fig. 1 are equivalent to the coupling systems composed of energy selective electron Carnot heat engines and coolers.

Next, we describe how to determine directions of thermal fluxes. The first case [Fig. 1(b)] is characterized by $\mu_c > \mu_h$. The tunnel at the energy level, E_{hc}, connects hot and cold reservoirs. If $E_{hc} > E^*_{hc}$, the FD distribution in

the hot reservoir is higher than the counterpart in the cold reservoir, implying that the electron flow will spontaneously travel from the hot reservoir to the cold reservoir. Since $E_{hc} > E^*_{hc}$ and $\mu_c < E^*_{hc}$ (Supplementary S-1), we can obtain $E_{hc} - \mu_c > 0$, and $E_{hc} - \mu_h > 0$. These two inequalities imply that a positive thermal flux leaves the hot reservoir and a positive thermal flux enters the cold reservoir. Next, because $T_c < T_m$, the energy level, E_{mc} must be lower than E^*_{mc}. Under this condition, the FD distribution at E_{mc} in the median reservoir is lower than the counterpart in the cold reservoir, implying that the electron flow will spontaneously move from the cold reservoir to the median reservoir, and that the continuity of the electron flow is satisfied.

Regarding signs of energy fluxes, only when $E_{mc} - \mu_c > 0$ and $E_{mc} - \mu_m > 0$, a positive thermal energy leaves the cold reservoir, and a positive thermal flux enters the median reservoir. At this juncture, the only remaining task is the comparison of magnitudes of μ_m and μ_c. According to analyses above, we should have $\mu_c < E^*_{mc}$. Finally, we obtain $\mu_c > \mu_m$ (Supplementary S-1), under which the cooler can work. The E_{mh} level should be designed such that the continuity of electron fluxes is guaranteed. Therefore, we are able to utilize this condition to determine E_{mh} numerically. Once having made this determination, we are able to obtain q_c exiting the cold reservoir and the thermal flux q_h leaving the hot reservoir. Subsequently, we are able to determine the cooling performance. This mechanism can work for thermal amplification processes as well if our interest lies in deliver thermal energy to the median reservoir.

The second case [Fig. 1(c)] is characterized by $\mu_c < \mu_h$ and we can design a cycle whose characteristics are similar to those in the first case, but the electron and thermal fluxes flow in the opposite direction (Supplementary S-2). Figure 1(c) can also be designed to work as a cooler or an amplifier. We also observe that $\mu_c < \mu_m$ (Supplementary S-2).

Discussion

Thermal electron-tunneling device as a cooler. When the thermal device works as a cooler, we can define the cooling modulus as $\varphi = q_c/q_h$. As $\Delta E \to 0$, we can obtain $q_{c/h}$ in a simplified form based on Eq. (2) as

$$q_{c/h} = \frac{2}{h}\Big\{\mp(E_{hc} - \mu_{c/h})[f_h(E_{hc}) - f_c(E_{hc})]\Delta E - (E_{m(c/h)} - \mu_{c/h})[f_m(E_{m(c/h)}) - f_{c/h}(E_{m(c/h)})]\Delta E\Big\}, \tag{3}$$

where symbols $\mp$ correspond to cases of subscripts c and h, respectively. Because continuity equations of electron fluxes satisfy $f_h(E_{hc}) - f_c(E_{hc}) = f_c(E_{mc}) - f_m(E_{mc}) = f_m(E_{mh}) - f_h(E_{mh})$, we obtain the cooling modulus as

$$\varphi = \frac{E_{mc} - E_{hc}}{E_{hc} - E_{mh}} = \frac{\delta_2}{\delta_1} - 1, \tag{4}$$

where $\delta_1 = E_{hc} - E_{mh}$ and $\delta_2 = E_{mc} - E_{mh}$. When E_{hc}, E_{mc}, and E_{mh} equal E^*_{hc}, E^*_{mc}, and E^*_{mh}, respectively, we obtain[29,30]

$$\varphi = \frac{E^*_{mc} - E^*_{hc}}{E^*_{hc} - E^*_{mh}} = \frac{(T_h - T_c)}{T_h}\frac{T_c}{(T_m - T_c)} \equiv \varphi_{rev}, \tag{5}$$

implying that electron transports via three tunnels are reversible, and the cooler yields a reversible performance, φ_{rev}.

From Eq. (4), we can conclude that δ_1 and δ_2 are two crucial independent parameters to determine the performance of the device. As indicated in Fig. 2(b), φ is required to be larger than zero by suitably selecting values of δ_1 and δ_2, lying within the shaded area confined by $\varphi = 0$ and $\varphi = \varphi_{rev}$. For ideal tunnels whose electron occupations of states are infinitesimally close to an equilibrium state and whose widths become infinitesimally small, reversible electron transports can be achieved (Supplementary S-3).

For non-ideal cases, tunnel energy levels deviate from E^*_{hc}, E^*_{mc}, and E^*_{mh} and their widths become finite. For purposes of illustrating performance characteristics, let us choose $T_h = 3\,K$, $T_m = 1.5\,K$, $T_c = 1\,K$, and $\mu_c/k = 10$, as shown in Fig. 3. The parameter μ_h/k will be optimally designed in the following discussion. The other parameter μ_m/k will be computed through electron-flux continuity equations.

Figure 3 reveals the performance of the thermal device as a cooler. The results in Fig. 3 are simultaneously determined by μ_c, μ_h, μ_m, E_{hc}, E_{mh}, E_{mc}, and ΔE. The parameter, μ_h, has been optimized for maximum q_c, while μ_m has been designed to satisfy continuity equations of electron fluxes (Method). Figure 3(a–c) show contour plots of the cooling modulus, φ, versus δ_1 and δ_2, parameterized in $\Delta E/k$ approaching $0\,K$, or equaling $0.1\,K$ and $0.5\,K$. Values of φ are seen to be approximately symmetrical to the point at $\delta_1/k = 0\,K$ and $\delta_2/k = 0\,K$. For $\mu_c > \mu_h$ [Fig. 1(b)], results show that $\delta_1 > 0$ and $\delta_2 > 0$, indicating that E_{mh} should be adjusted to the lowest. For $\mu_c < \mu_h$ [Fig. 1(c)], we find that $\delta_1 < 0$ and $\delta_2 < 0$, implying that E_{mh} should become the highest. For this configuration, the electron flux and the energy flux cross each other.

In Fig. 3(a), $\Delta E/k \to 0$, φ appears to be a monotonic function of δ_1 and δ_2. When the maximum value of the cooling modulus, $\varphi_{\max}$, approaches unity, which is computed from Eq. (5) for ideal cases, the model will exhibit its reversible performances. When the tunnel width becomes finite [Fig. 3(b,c)], contours show maxima. For example, when $\Delta E/k = 0.5\,K$, φ_{max} approaches 0.580, which is lower than the reversible value. The area enclosed by the innermost contour in Fig. 3(b) is smaller than that in Fig. 3(c), suggesting that it is easier to select δ_1 and δ_2 to achieve $\varphi_{\max}$ in the case shown in Fig. 3(c). As $\Delta E/k$ widens, tunnels lose their abilities to select electrons, leading to electron-transport irreversibilities, thus lowering φ values.

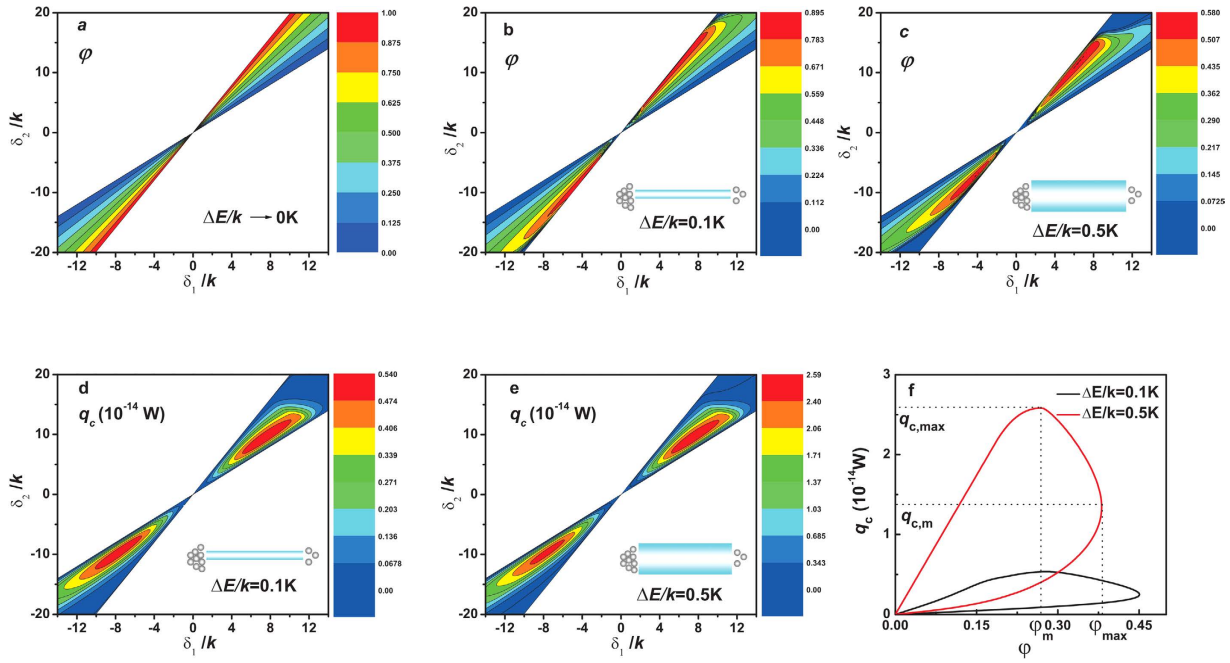

Figure 3. Cooling performance of the proposed device. (**a**–**c**) Cooling modulus, φ, as a function of δ_1 and δ_2, parametrized in the tunnel width, $\Delta E/k$. (**a**) As $\Delta E/k$ approaches zero, the device attains the reversible performance. (**b**,**c**) As $\Delta E/k$ increases, the irreversibility related to the electron transport increases, causing φ to decrease. (**d**,**e**) The cooling rate, q_c, as a function of δ_1 and δ_2. We are able to identify $q_{c,max}$ in the operable regime. (**f**) q_c versus φ after optimization of q_c with respect to δ_1. There exists a negative slope arc segment on which q_c decreases as φ increases. This trend appears more pronounced for $\Delta E/k = 0.5\,K$.

The value of q_c increases as $\Delta E/k$ increases, but the irreversibility also increases [Fig. 3(d,e)]. However, we can find that maximum q_c exists with respect to δ_1 and δ_2. Alternatively, we optimize q_c with respect to δ_1 and obtain q_c as a function of φ [Fig. 3(f)]. The q_c versus φ curve is a closed loop passing through the origin. On the curve, there exists a φ_{max} whose corresponding cooling rate is $q_{c,m}$, and a maximum cooling rate $q_{c,max}$ whose corresponding coefficient is φ_m. Thus, the ranges of the cooling modulus and the cooling rate must be constrained by $\varphi_m \le \varphi \le \varphi_{max}$ and $q_{c,m} \le q_c \le q_{c,max}$. Clearly, φ_{max} and $q_{c,max}$ determine upper bounds of the cooling modulus and the cooling rate, while φ_m and $q_{c,m}$ give lower bounds of the optimized values of both. When the cooler is operated in the optimally working region with negative slope arc segments, both the cooling rate, q_c, and the rate of the entropy production of three electron reservoirs, $\sigma = q_m/T_m - q_h/T_h - q_c/T_c$, are of monotonically decreasing functions of the cooling modulus, φ. For example, it can be obtained from the negative slope arc segment with $\Delta E/k = 0.5$ K in Fig. 3(f) that when $\varphi = 0.268$, $q_c = 2.582 \times 10^{-14}\,W$ and $\sigma = 2.357 \times 10^{-14}\,W/K$; when $\varphi = 0.333$, $q_c = 2.204 \times 10^{-14}\,W$ and $\sigma = 1.470 \times 10^{-14}\,W/K$. Thus, one should simultaneously consider both the cooling modulus and the cooling rate in the practical design of devices.

Thermal electron-tunneling device as an amplifier. When the thermal device works as an amplifier, the amplification ratio $\psi = q_m/q_h = \delta_2/\delta_1 = \varphi + 1$. Following similar arguments described for coolers, as $\Delta E/k$ approaches zero and E_{hc}, E_{mc}, and E_{mh} equal E^*_{hc}, E^*_{mc}, and E^*_{mh}, respectively, we can derive the amplifier ratio as $\psi_{rev} = (1 - T_c/T_h)T_m/(T_m - T_c)$[31], yielding the reversible performance. For general cases, one can discuss the performance of an amplifier by using the similar method analyzed for a cooler. This shows that such a device can behave as a cooler or an amplifier, depending on our interest in extracting thermal energy from the cold reservoir, or pumping thermal energy into the median reservoir.

The proposed model is one of thermal spontaneous conversion devices that have been rarely searched. By optimizing the energy levels of all tunnels in the FD sense, we are capable of manipulating flux-directions at our disposal, constructing either coolers or thermal amplifiers in the absence of electrical power inputs, and concurrently reducing flux irreversibilities to achieve high thermal performances. The pioneering investigation on the proposed model can open a new avenue for building practical thermal electron-tunneling devices and have potentially significant applications where thermal manipulation at micro/nano levels is required.

Methods

All the integrals are numerically performed by using the Gaussian Quadrature. For given values of μ_c and ΔE, there are five unknown parameters, namely, μ_h, μ_m, E_{hc}, E_{mh}, and E_{mc}. The numerical method to evaluate the device performance is summarized as follows: (1) By transforming the abscissa (horizontal, δ_1) and the ordinate (vertical, δ_2) into $E_{hc} = \delta_1 + E_{mh}$ and $E_{mc} = \delta_2 + E_{mh}$, we are left with three unknowns: μ_h, μ_m, and E_{mh}. (2) When μ_h is further given, the continuity equations $n_{ch}(\mu_m, E_{mh}) = n_{mc}(\mu_m, E_{mh})$ and $n_{hm}(\mu_m, E_{mh}) = n_{mc}(\mu_m, E_{mh})$ are

numerically computed self-consistently to obtain μ_m and E_{mh}. For solving these two nonlinear integral equations, we loop the two unknown variables. One loop is nested in the other loop. The inner loop is stopped if $n_{ch}(\mu_m, E_{mh}) = n_{mc}(\mu_m, E_{mh})$ is valid, and then we check the other equation. If $n_{ch}(\mu_m, E_{mh}) = n_{mc}(\mu_m, E_{mh})$ is not valid, we go back to the outer loop. This procedure is repeated until two continuity equations are valid. (3) Following the above calculation, we optimize μ_h such that the thermal energy q_c reaches maxima. (4) With the help of all parameters precisely determined, the cooling modulus φ can be obtained. In semiconductors, the position of μ relative to the band structure is usually controlled by doping with donor and acceptor impurities[10]. The biased chemical potentials can also be generated by the external electric powers, but the consumption of electricity must be considered to evaluate the device performance.

References

1. Helbling, E. W., Banaszak, A. T. & Villafañe, V. E. Global change feed-back inhibits cyanobacterial photosynthesis. *Sci. Rep.* **5,** 14514 (2015).
2. Yamori, W., Shikanai, T. & Makino, A. Photosystem I cyclic electron flow via chloroplast NADH dehydrogenase-like complex performs a physiological role for photosynthesis at low light. *Sci. Rep.* **5,** 13908 (2015).
3. Bergenfeldt, C. *et al.* Hybrid microwave-cavity heat engine. *Phys. Rev. Lett.* **112,** 076803 (2014).
4. Hardal, A. Ü. C. & Müstecaplıoglu, Ö. E. Superradiant quantum heat engine. *Sci. Rep*. **5,** 12953 (2015).
5. Levy, A. & Kosloff, R. Quantum absorption refrigerator. *Phys. Rev. Lett*. **108,** 070604 (2012).
6. Li, B., Wang, L. & Casati, G. Thermal diode: Rectification of heat flux. *Phys. Rev. Lett*. **93,** 184301 (2004).
7. Chang, C. W., Okawa, D., Majumdar, A. & Zettl, A. Solid-state thermal rectifier. *Science* **314,** 1121–1124 (2006).
8. Xu, W., Zhang, G. & Li, B. Interfacial thermal resistance and thermal rectification between suspended and encased single layer graphene. *J. Appl. Phys.* **116,** 134303 (2014).
9. Lappala, A., Zaccone, A. & Terentjev, E. M. Ratcheted diffusion transport through crowded nanochannels. *Sci. Rep.* **3,** 3103 (2013).
10. Sze, S. M. *Physics of semiconductor devices* (Wiley, New York, 1981).
11. Humphrey, T. E., Newbury, R., Taylor, R. P. & Linke, H. Reversible quantum Brownian heat engines for electrons. *Phys. Rev. Lett.* **89,** 116801 (2002).
12. Wang, L. & Li, B. Thermal logic gates: Computation with phonons. *Phys. Rev. Lett.* **99,** 177208 (2007).
13. Li, B., Wang, L. & Casati, G. Negative differential thermal resistance and thermal transistor. *Appl. Phys. Lett.* **88,** 143501 (2006).
14. Humphrey, T. E. & Linke, H. Reversible thermoelectric nanomaterials. *Phys. Rev. Lett.* **94,** 096601 (2005).
15. Su, S., Guo, J., Su, G. & Chen, J. Performance optimum analysis and load matching of an energy selective electron heat engine. *Energy* **44,** 570–575 (2012).
16. Davies, J. H. *The physics of low-dimensional semiconductors: an introduction* (Cambridge university press, 1998).
17. Al-Dirini, F. *et al.* Highly effective coductance modulation in planar silicene field effect devices due to buckling. *Sci. Rep.* **5,** 14815 (2015).
18. Luo, X. *et al.* A theoretical study on the performances of thermoelectric heat engine and refrigerator with two-dimensional electron reservoirs. *J. Appl. Phys.* **115,** 244306 (2014).
19. O'Dwyer, M. F., Humphrey, T. E., Lewis, R. A. & Zhang, C. Efficiency in nanometre gap vacuum thermionic refrigerators. *J. Phys. D: Appl. Phys.* **42,** 035417 (2009).
20. Luo, X. *et al.* The impact of energy spectrum width in the energy selective electron low-temperature thermionic heat engine at maximum power. *Phys. Lett. A* **377,** 1566–1570 (2013).
21. Agarwal, A. & Muralidharan, B. Power and efficiency analysis of a realistic resonant tunneling diode thermoelectric. *Appl. Phys. Lett.* **105,** 013104 (2014).
22. Li, C., Zhang, Y., Wang, J. & He, J. Performance characteristics and optimal analysis of a nanosized quantum dot photoelectric refrigerator. *Phys. Rev. E* **88,** 062120 (2013).
23. Nakpathomkun, N., Xu, H. Q. & Linke, H. Thermoelectric efficiency at maximum power in low-dimensional systems. *Phys. Rev. B* **82,** 235428 (2010).
24. Giazotto, F. & Martnez-Pérez, M. J. The Josephson heat interferometer. *Nature* **492,** 401–405 (2012).
25. Hechenblaikner, G. *et al.* How cold can you get in space? Quantum physics at cryogenic temperatures in space. *New J. Phys.* **16,** 013058 (2014).
26. Wellstood, F. C., Urbina, C. & Clarke, J. Hot-electron effects in metals. *Phys. Rev. B* **49,** 5942–5955 (1994).
27. O'Dwyer, M. F., Humphrey, T. E. & Linke, H. Concept study for a high-efficiency nanowire based thermoelectric. *Nanotechnology* **17,** S338–S343 (2006).
28. Luo, X., Liu, N., He, J. & Qiu, T. Performance analysis of a tunneling thermoelectric heat engine with nano-scaled quantum well. *Appl. Phys. A* **117,** 1031–1039 (2014).
29. Yan, Z. & Chen, J. An optimal endoreversible three-heat-source refrigerator. *J. Appl. Phys.* **65,** 1–4 (1989).
30. Correa, L. A., Palao, J. P., Alonso, D. & Adesso, G. Quantum-enhanced absorption refrigerators. *Sci. Rep.* **4,** 3949 (2014).
31. Chen, J. & Yan, Z. Unified description of endoreversible cycles. *Phys. Rev. A* **39,** 4140–4147 (1989).

Acknowledgements

This work has been supported by the National Natural Science Foundation (No. 11175148), 973 Program (No. 2012CB619301), and China Postdoctoral Science Foundation (No. 2015M580964), People's Republic of China.

Author Contributions

J.C. designed the thermal electron-tunneling device. S.S. performed the computation. T.-M.S. took part in writing the manuscript. All the authors discussed the results and improved the manuscript.

Additional Information

Supplementary information accompanies this paper at http://www.nature.com/srep

Competing financial interests: The authors declare no competing financial interests.

How to cite this article: Su, S. *et al.* Thermal electron-tunneling devices as coolers and amplifiers. *Sci. Rep.* **6**, 21425; doi: 10.1038/srep21425 (2016).